Orbiting blobs in accretion discs in the era of high angular resolution and polarimetry

Vladimír Karas

Astronomical Institute, Prague

in collaboration with

Andreas Eckart (University of Cologne and MPI f. Radioastronomy in Bonn)

Michal Zajaček (Polish Acad. of Sci. in Warsaw and Masaryk Univ. in Brno)

Session on “eXTP – enhanced X-ray Timing and Polarimetry Mission”, id. #549

16th Marcel Grossmann Meeting **5-10 July 2021 (on-line)**

Rotation of ionized gas in M84

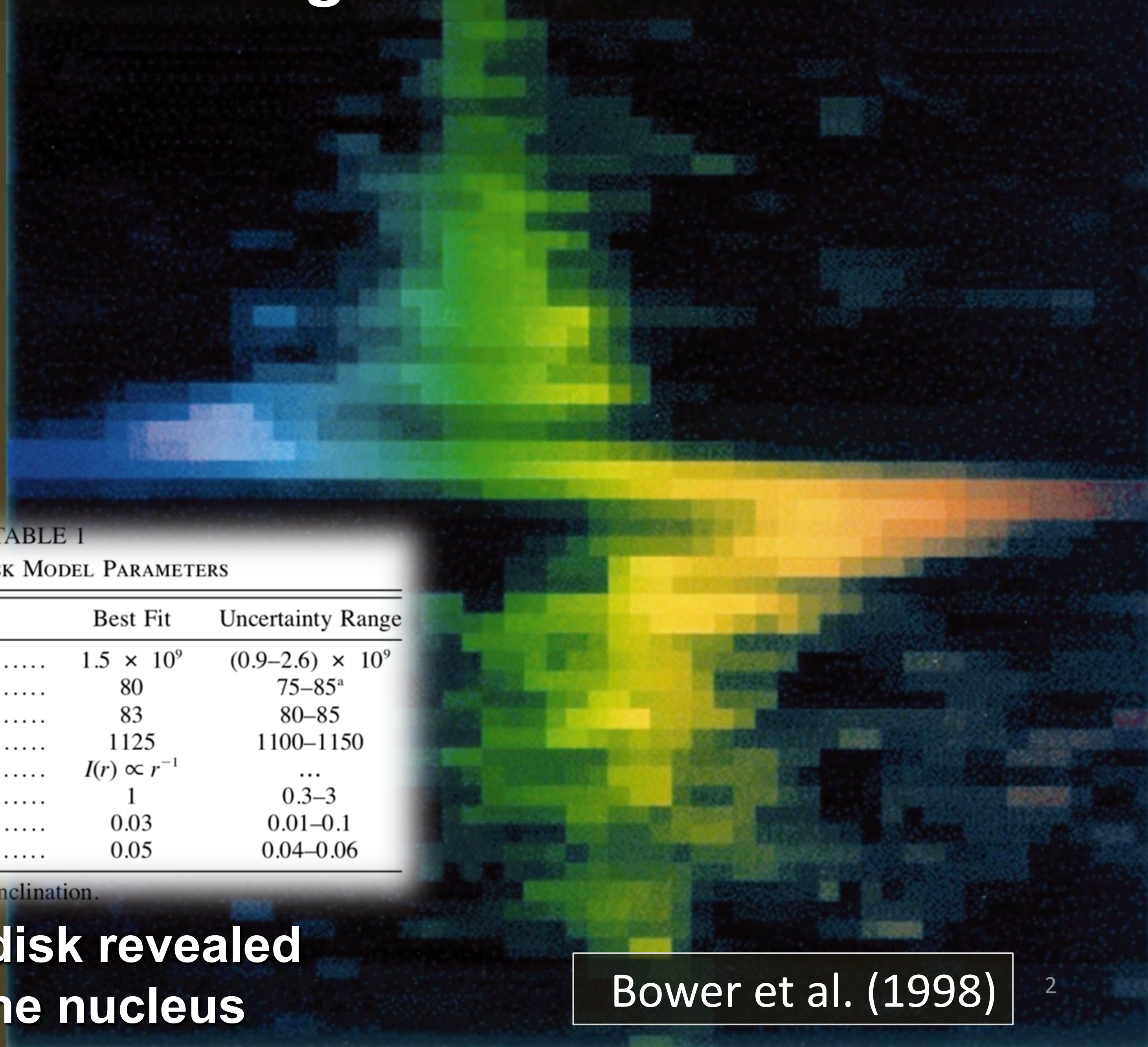

TABLE 1

KEPLERIAN DISK MODEL PARAMETERS

Parameter	Best Fit	Uncertainty Range
Black hole mass ($M_\odot$)	1.5×10^9	$(0.9–2.6) \times 10^9$
Disk inclination (deg)	80	75–85[a]
Disk P.A. (deg)	83	80–85
Gas systemic velocity (km s^{-1})	1125	1100–1150
Intensity law	$I(r) \propto r^{-1}$	...
$I(r)$ inner radius (pc)	1	0.3–3
$V(r)$ inner radius (pc)	0.03	0.01–0.1
PSF σ (arcsec)	0.05	0.04–0.06

[a] Lower mass requires lower inclination.

Nuclear gas disk revealed ~ 8 pc from the nucleus

Bower et al. (1998)

Rotation of ionized gas in NGC 4261

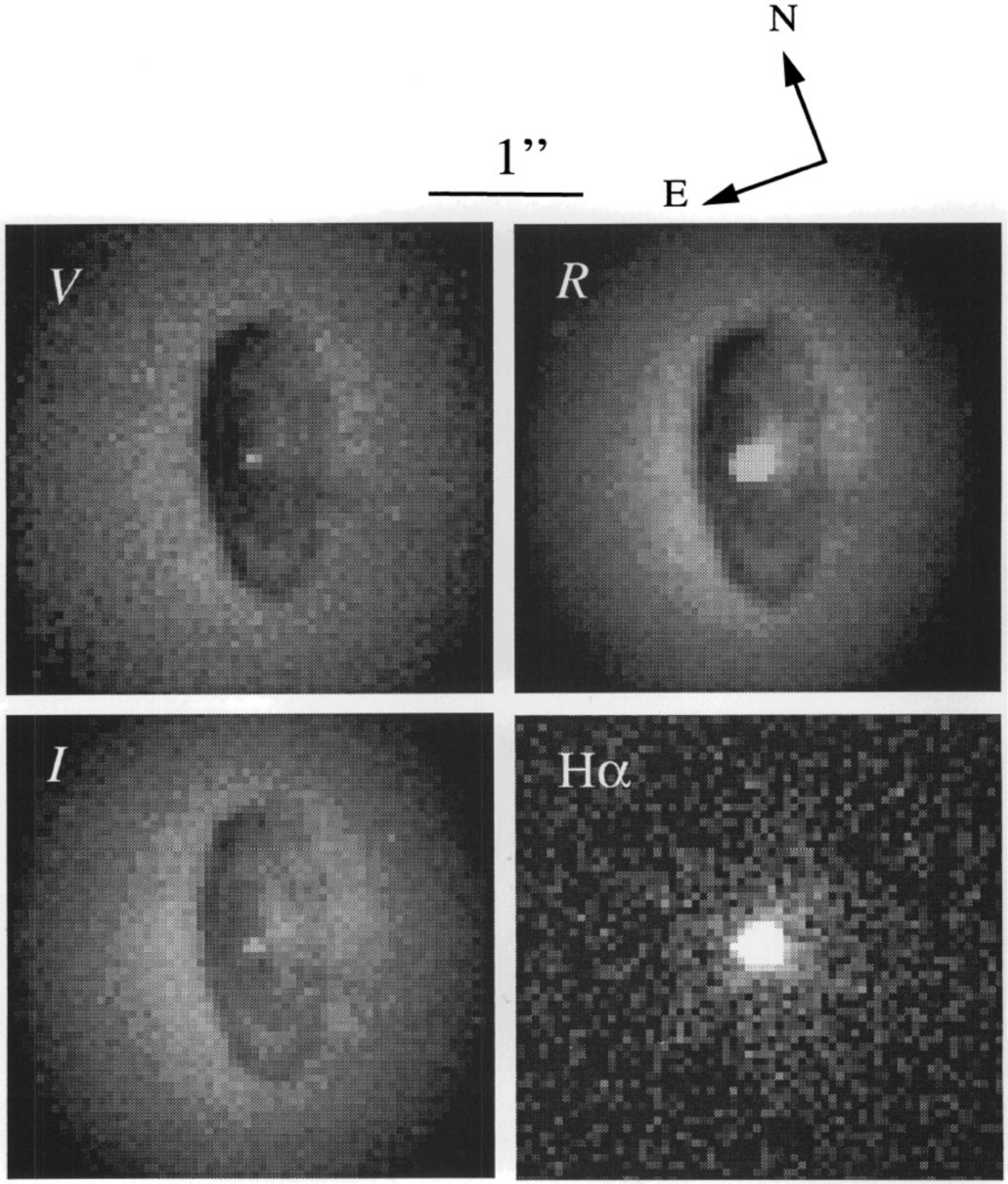

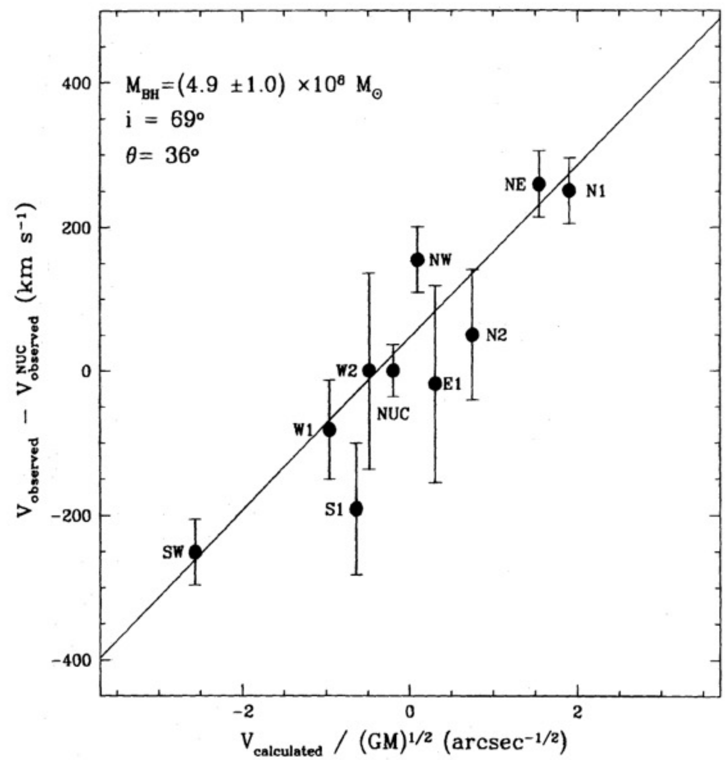

FIG. 11.—Predicted velocities vs. the observed velocities for the best-fitting Keplerian model. The data can be fitted by a straight line, implying that the gas is in Keplerian motion. The predicted velocities, derived from the model for $(GM_{BH})^{1/2} = 1$, are in units of arcsec$^{-1/2}$.

Ferrarese et al. (1996)

Orbital dynamics of maser sources

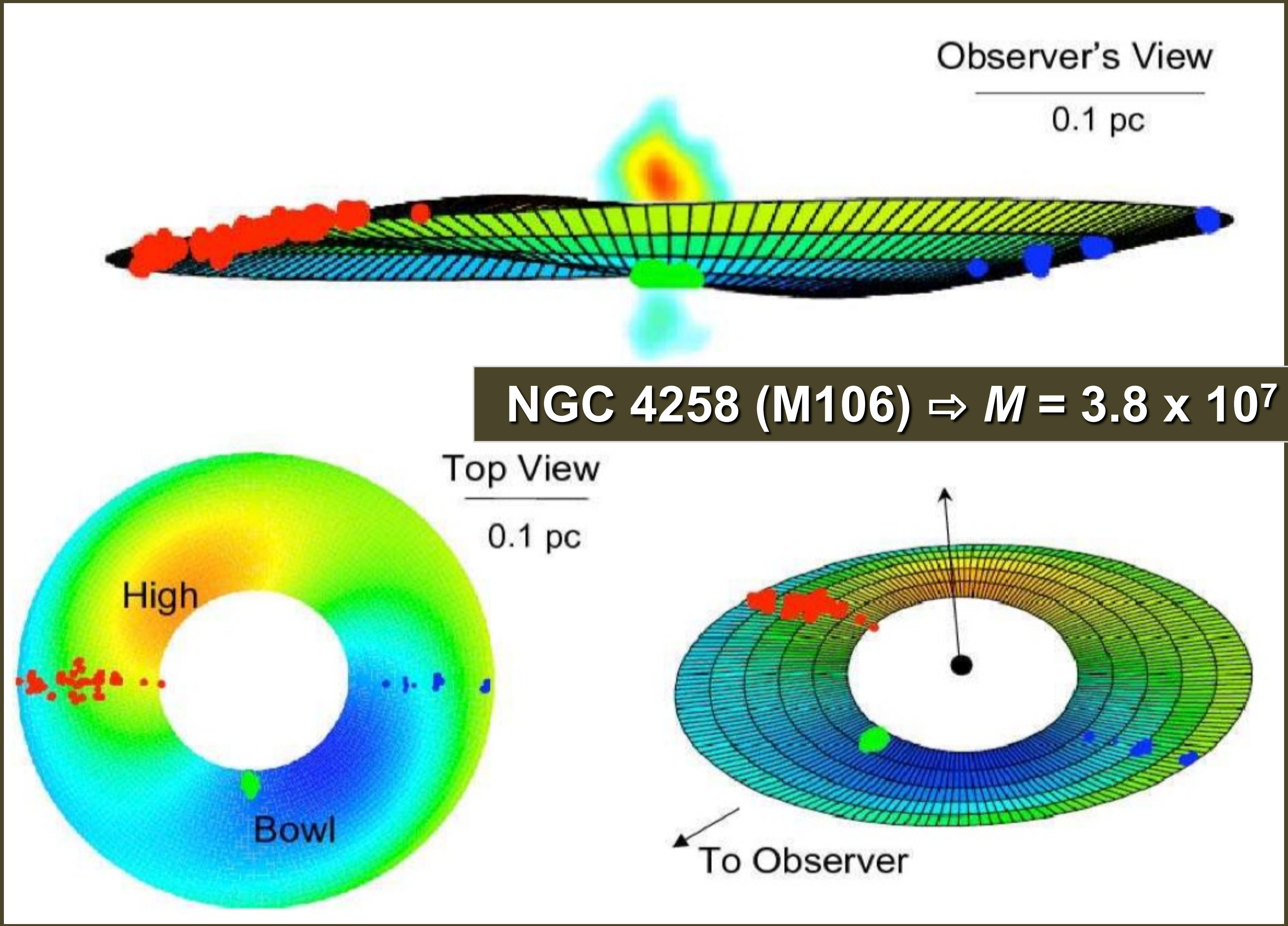

NGC 4258 (M106) ⇨ M = 3.8 x 10^7 M_S

Miyoshi et al. (1995); Herrnstein et al. (2005); Moran (2008)

Reverberation mapping of BLR AGN

C. Ricci http://www.isdc.unige.ch/~ricci

$$M_{\rm BH} = \frac{f r \Delta V^2}{G}$$

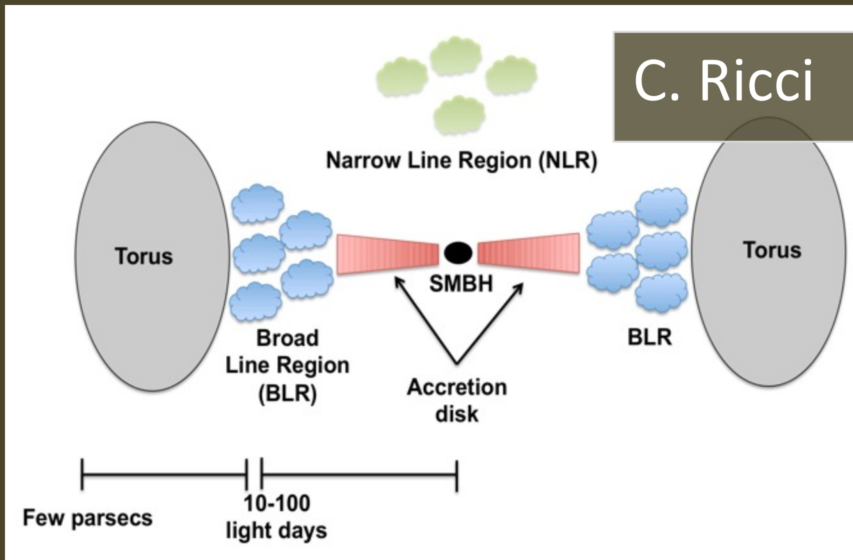

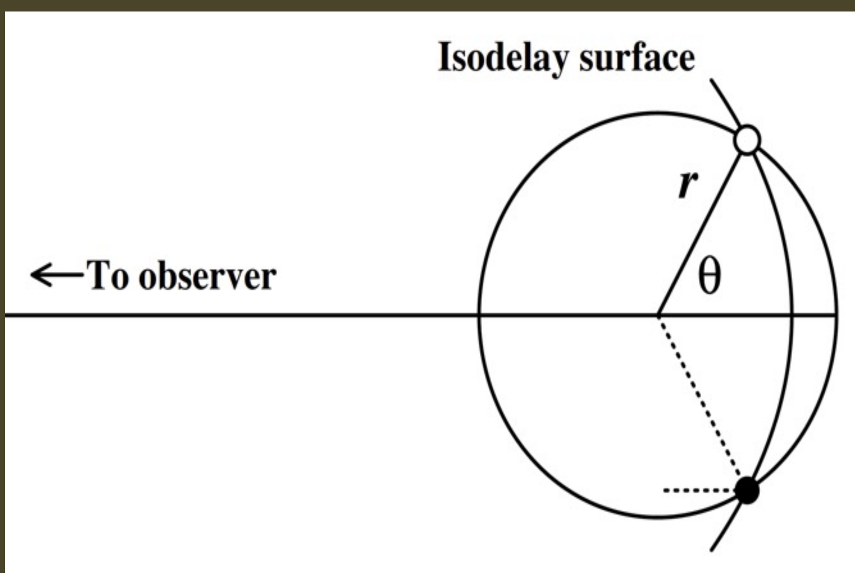

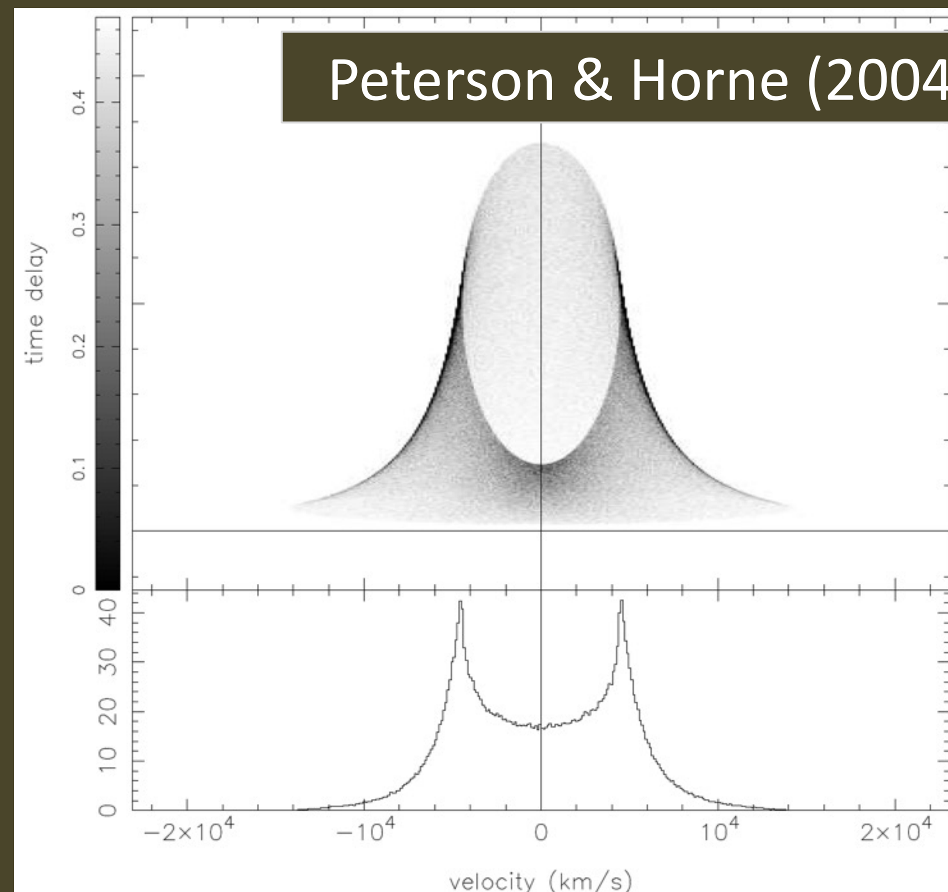

Peterson & Horne (2004)

Polarization mapping of BLR AGN

Afanasiev & Popovic (2015)

The Astrophysical Journal Letters, 800:L35 (4pp), 2015 February 20

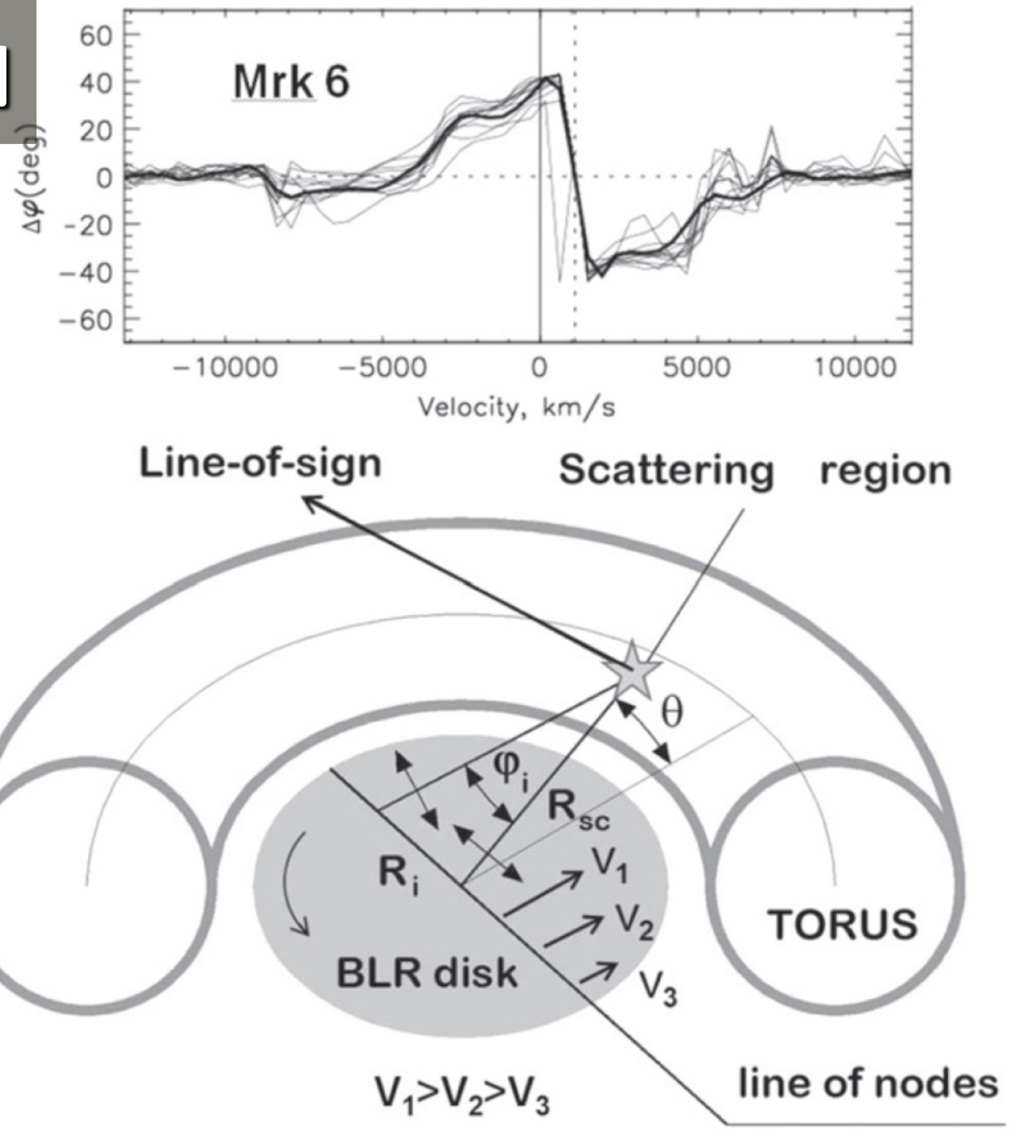

Figure 1. Our assumed scattering geometry is indicated in the lower panel of the figure, and the observed dependence of polarization angle ($\Delta\varphi$) vs. velocities in the Hα line profile of Mrk 6 is shown in the upper panel of the figure (see Afanasiev et al. 2014).

SMBH mass from bright flares

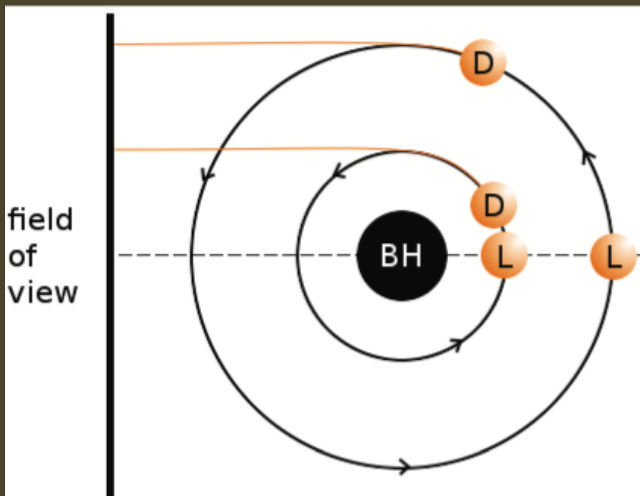

$$g = \frac{\nu_0}{\nu_e} = \frac{p_{0t}}{p_i U^i} = \frac{E_\infty}{p_i U^i}$$

Table 1. Basic parameters of the simulations.

Parameter	Values	Description
a	0.5	BH spin
M	1	BH mass
i	$5°, 10°,..., 90°$	Inclination
D_0	$0.5\,r_g, 1\,r_g,..., 5.0\,r_g$	Size of the blob
R_0	$6\,r_g, 8\,r_g,..., 24\,r_g$	Blob's radial position
ϕ_0	90	Starting azimuth angle
n_e	1	Electron number density
R_{max}	$40\,r_g$	Max. domain radius
Nx	150	Resolution in pixels
frames	100	Time frames per orbit
step	$0.1\,r_g$	Step along geodesics

$$P_T = 310(R^{3/2} + a)M_7 = 49.3\,P_g \times M_7$$

Dovčiak et al. (2004); Karssen et al. (2017)

SMBH mass from bright flares

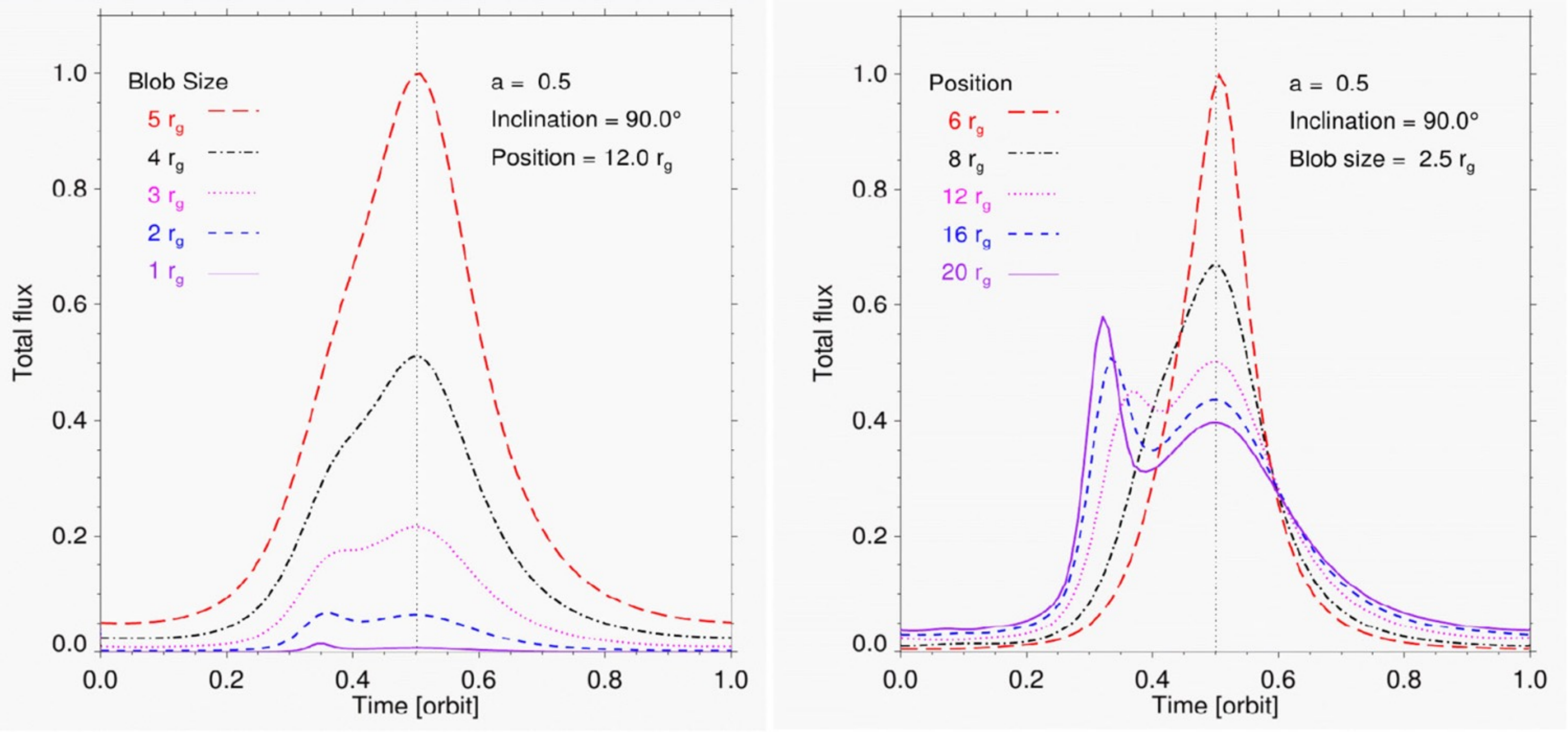

Karssen et al. (2017); Eckart et al. (2018)

SMBH mass from bright flares

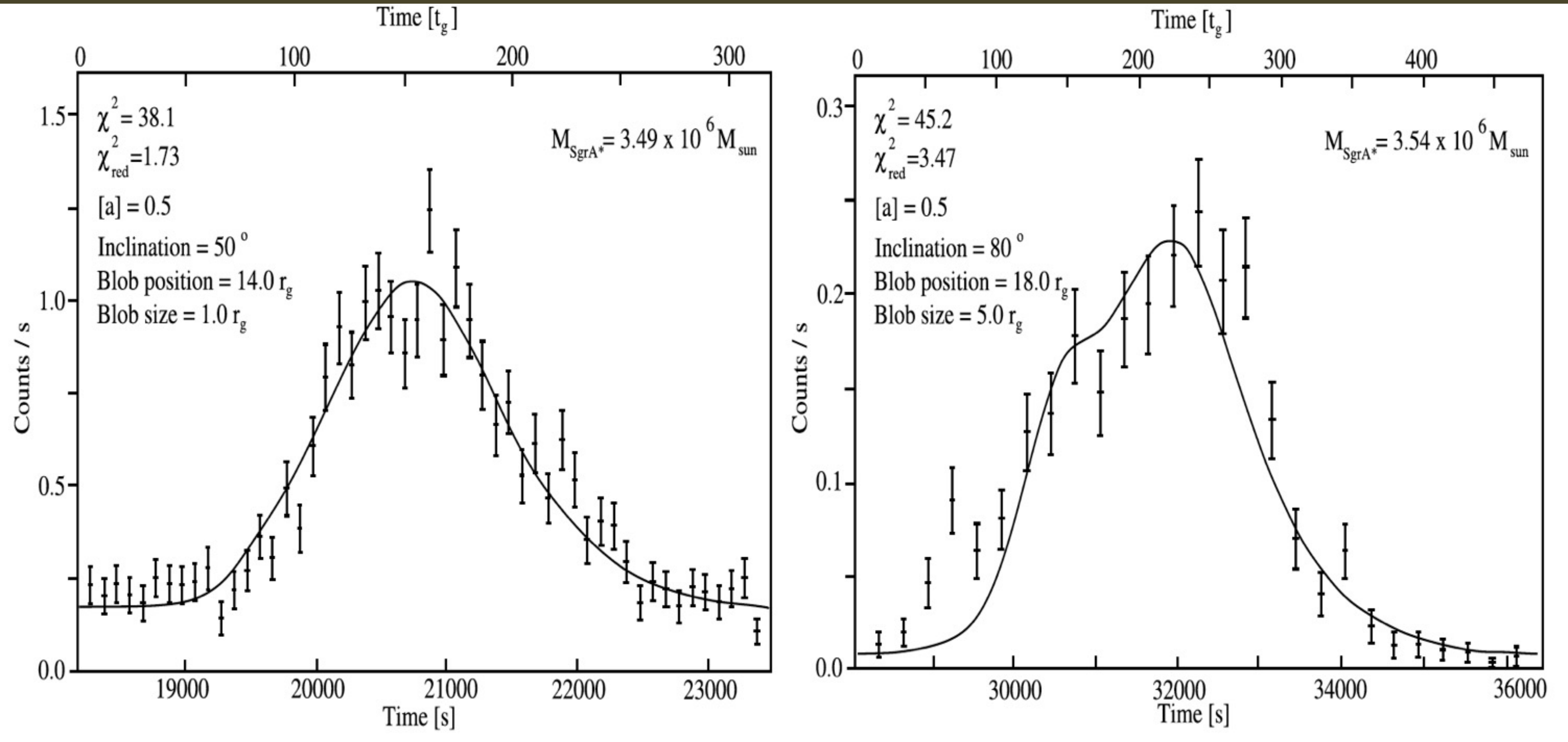

Karssen et al. (2017); Eckart et al. (2018)

SMBH mass from bright flares

Table 2. The median values of the mass model parameters M, i, R_0 and D_0 as well as the corresponding maximum amplification factor $\mathrm{Amp}_{\mathrm{max}}$.

Flare	$M[10^6\,\mathrm{M}_\odot]$	$i[^\circ]$	$R_0[r_g]$	$D_0[r_g]$	$\mathrm{Amp}_{\mathrm{max}}$
Baganoff et al. (2001)	$4.86^{+6.80}_{-2.41}$	46.47	15.69	2.85	25
Porquet et al. (2003)	$3.45^{+4.07}_{-1.43}$	55.40	12.43	2.59	39
Porquet et al. (2008)	$3.13^{+3.81}_{-1.24}$	49.16	14.24	2.84	32
Nowak et al. (2012)	$3.54^{+1.02}_{-1.01}$	69.52	17.90	3.60	51
Median	3.49 ± 0.20				
All flare fit	$3.94^{+4.85}_{-1.86}$				
Mossoux et al. (2015) (Epic)	$3.18^{+5.56}_{-2.57}$	60.68	14.14	3.06	49

Karssen et al. (2017); Eckart et al. (2018)

Light curves from orbiting blobs

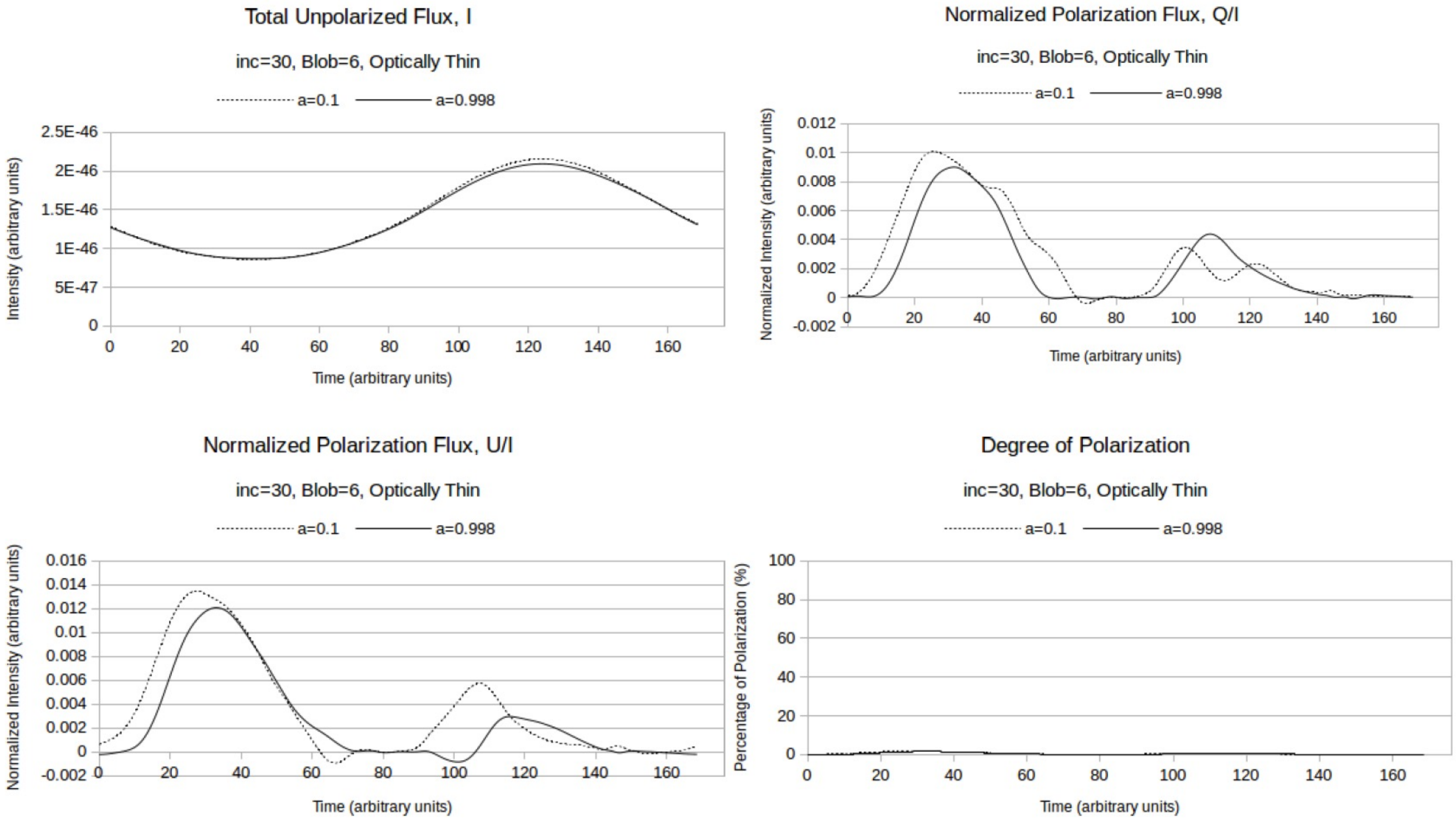

Figure 8.9: An optically thin ($\rho = 10^{-10}\,\mathrm{g\,cm^{-3}}$), spherical blob ($6\ \mathrm{r_g}$) positioned at $9\ \mathrm{r_g}$. Light curves of an orbit is observed at $30°$ for spin 0.1 and 0.998. The parameters I (total intensity), Q/I and U/I (normalized polarization flux) and δ (polarization degree) are plotted.

Munawwar Khanduwala (2018)

Conclusions. Energy shifts of radiation from accreting black holes may be caused by the fast orbital motion and the gravitational redshift near the event horizon.

Individual clumps of matter experience the effects of general relativity as they gradually sink into a deep potential well. An episodic supply of material is maintained by tidal disruption events and the emerging radiation is modulated in the X-ray domain and in longer wavelengths.

Changes of polarization properties of the observed signal exhibit a specific dependence on energy.

SMBH mass from bright flares

Table 3. Mass estimates of the Seyfert I galaxy RE J1034+396 with different methods in a chronological order.

Publication	Mass	Method
Gierliński et al. (2008)	$6.3 \times 10^5\,M_\odot$	H β
Gierliński et al. (2008)	$3.6 \times 10^7\,M_\odot$	[O III]
Gierliński et al. (2008)	$(8 \times 10^6 - 9 \times 10^7)\,M_\odot$	ISCO
Bian & Huang (2010)	$(1–4) \times 10^6\,M_\odot$	$M - \sigma_*$
Bian & Huang (2010)	$(1–4) \times 10^6\,M_\odot$	H β
Jin et al. (2012)	$1.7 \times 10^6\,M_\odot$	H β
This paper	$1.421 \times 10^6\,M_\odot$	hotspot

Karssen et al. (2017); Eckart et al. (2018)

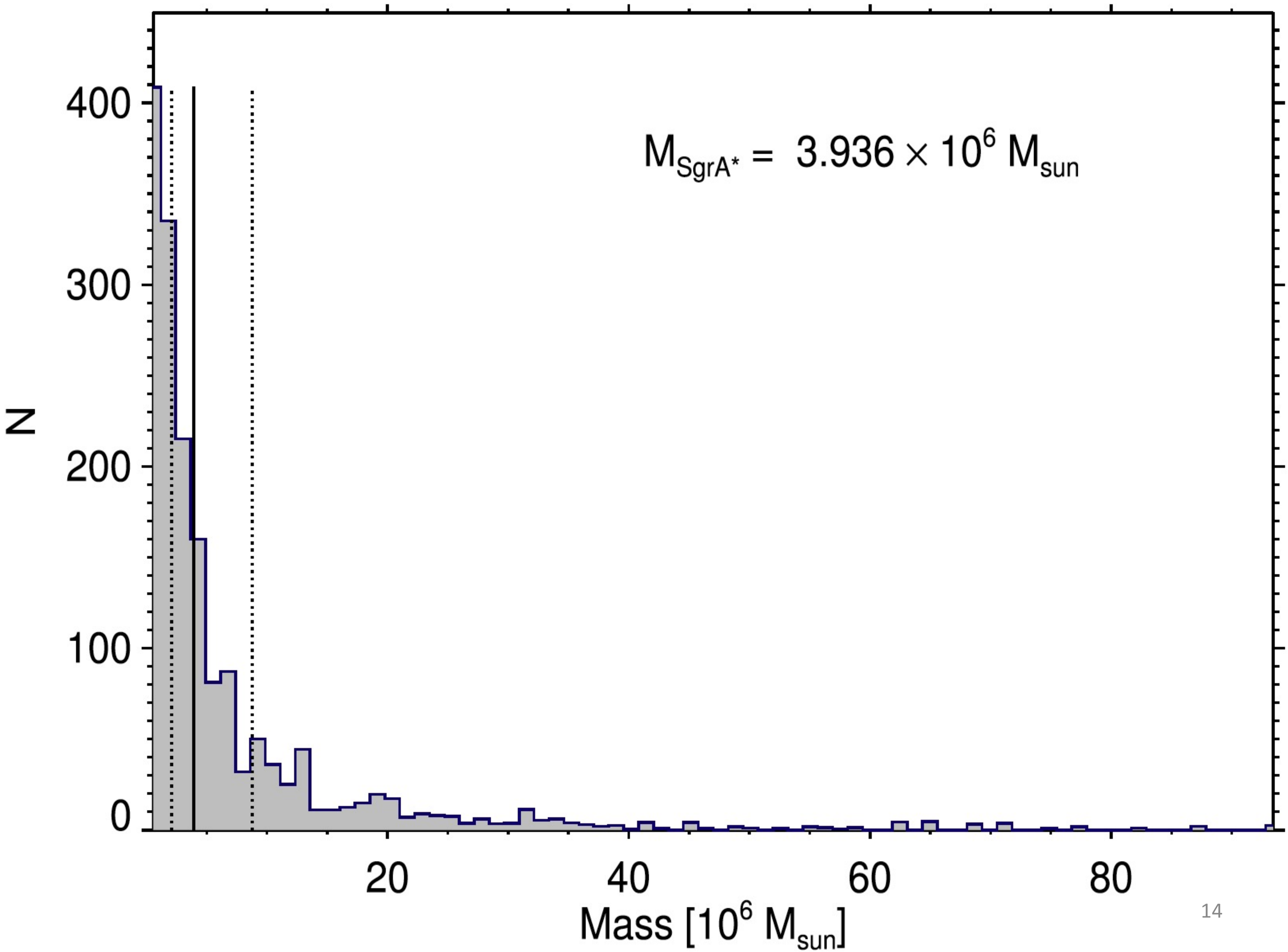

$M_{SgrA^*} = 3.936 \times 10^6 M_{sun}$
N
400
300
200
100
0
20
40
60
80
Mass [$10^6 M_{sun}$]

Rotation of ionized gas in M84

ABSTRACT

We present optical long-slit spectroscopy of the nucleus of the nearby radio galaxy M84 (NGC 4374 = 3C 272.1) obtained with the Space Telescope Imaging Spectrograph aboard the *Hubble Space Telescope*. Our spectra reveal that the nuclear gas disk seen in the Wide Field Planetary Camera 2 imaging by Bower et al. is rotating rapidly. The velocity curve has an S-shape with a peak amplitude of 400 km s^{-1} at $0''.1$ = 8 pc from the nucleus. To model the observed gas kinematics, we construct a thin Keplerian disk model that fits the data well if the rotation axis of the gas disk is aligned with the radio jet axis. These models indicate that the gasdynamics are driven by a nuclear compact mass of $1.5 \times 10^9\ M_\odot$ with an uncertainty range of $(0.9\text{–}2.6) \times 10^9\ M_\odot$, and that the inclination of the disk with respect to the plane of the sky is 75°–85°. Of this nuclear mass, only $\leq 2 \times 10^7\ M_\odot$ can possibly be attributed to luminous mass. Thus, we conclude that a dark compact mass (most likely a supermassive black hole) resides in the nucleus of M84.

Subject headings: galaxies: active — galaxies: elliptical and lenticular, cD — galaxies: individual (M84) —

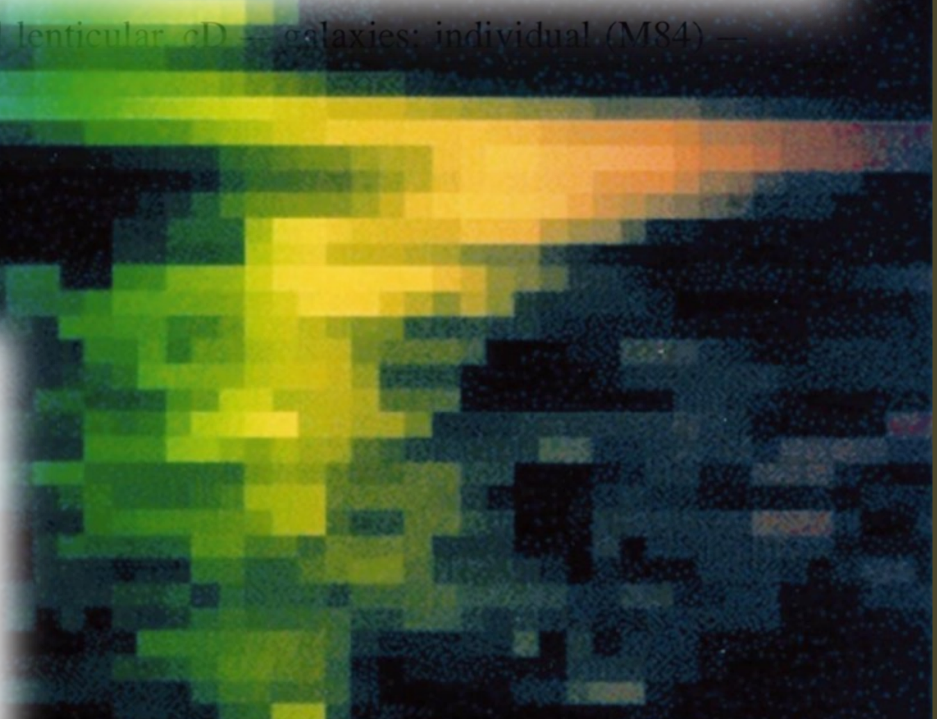

TABLE 1

KEPLERIAN DISK MODEL PARAMETERS

Parameter	Best Fit	Uncertainty Range
Black hole mass ($M_\odot$)	1.5×10^9	$(0.9\text{–}2.6) \times 10^9$
Disk inclination (deg)	80	75–85[a]
Disk P.A. (deg)	83	80–85
Gas systemic velocity (km s^{-1})	1125	1100–1150
Intensity law	$I(r) \propto r^{-1}$	...
$I(r)$ inner radius (pc)	1	0.3–3
$V(r)$ inner radius (pc)	0.03	0.01–0.1
PSF σ (arcsec)	0.05	0.04–0.06

[a] Lower mass requires lower inclination.

Bower et al. (1998)